Bioresource Technology 289 (2019) 121697

Contents lists available at ScienceDirect

Bioresource Technology

journal homepage: www.elsevier.com/locate/biortech

Evolutions of different microbial populations and the relationships with matrix properties during agricultural waste composting with amendment of iron (hydr)oxide nanoparticles

Lihua Zhang[a,b], Haoran Dong[a,b], Yuan Zhu[a,b], Jiachao Zhang[c], Guangming Zeng[a,b,*], Yujie Yuan[d], Yujun Cheng[a,b], Long Li[a,b], Wei Fang[a,b]

[a] College of Environmental Science and Engineering, Hunan University, Changsha 410082, PR China
[b] Key Laboratory of Environmental Biology and Pollution Control, Hunan University, Ministry of Education, Changsha 410082, PR China
[c] College of Resources and Environment, Hunan Agricultural University, Changsha 410082, PR China
[d] Institute of Hydroecology, Ministry of Water Resources and Chinese Academy of Sciences, Wuhan 430079, PR China

GRAPHICAL ABSTRACT

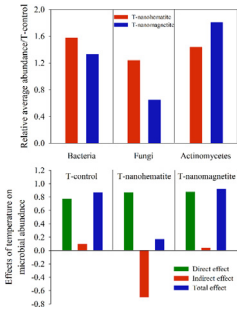

ARTICLE INFO

Keywords:
Composting
Microbial populations
Fe (hydr)oxide nanoparticles
Redundancy analysis
Partial least-squares path modeling

ABSTRACT

This study investigated the evolutions of different microbial populations and multivariate relationships between their abundances and environmental variables during composting with amendment of Fe (hydr)oxide nanoparticles. Piles treated with nanohematite and nanomagnetite were denoted as T-nanohematite and T-nanomagnetite, and another one was T-control. It was found that nanohematite more effectively increased bacteria and fungi abundances with 1.24 ~ 1.58 times average value of T-control, while nanomagnetite was more useful to actinomycetes. As the most significant variable, the total effect of temperature in T-control and T-nanomagnetite was increased to 0.87 and 0.92, respectively, because both the direct and indirect effects were positive, while it in T-nanohematite was reduced to 0.18 by the negative indirect effect. Partial redundancy analysis suggested that each microbial abundance shared different relationships with composting parameters. Overall, actinomycetes was more sensitive to changes of composting parameters than bacteria and fungi.

1. Introduction

With the rising of demands for varieties of fields, including commercial, industrial, agricultural, medical and electrical, manufactured nanoparticles (NPs) have been widely used. The worldwide utilization of NPs is expected to increase from 225,060 metric tons in

* Corresponding author at: College of Environmental Science and Engineering, Hunan University, Changsha 410082, PR China.
E-mail address: zgming@hnu.edu.cn (G. Zeng).

https://doi.org/10.1016/j.biortech.2019.121697
Received 12 May 2019; Received in revised form 20 June 2019; Accepted 21 June 2019
Available online 25 June 2019
0960-8524/

2014 to 584,984 metric tons in 2019 and will continue to grow in the future (Yi et al., 2018; Gong et al., 2009). Consequently, environmental impacts of NPs were intensively focused and reported (Wang et al., 2018; Yang et al., 2018). For example, TiO_2 NPs, CuO NPs and AgNPs were found to be potentially harmful to the environment, such as showing toxicity to aquatic organisms, reducing enzyme activities and microbial biomass carbon, changing the microbial community composition, etc. (Li et al., 2018; Xu et al., 2015; Asadishad et al., 2018; He et al., 2018).

Fe (hydr)oxide NPs have also been widely used in many fields, including medical, environmental, etc. (Xu et al., 2012; Zhou et al., 2018), among which hematite NPs and magnetite NPs were very popular because of their properties as a nutritional Fe source and their small size, high surface area/volume ratio, high separation convenience, low cost, and absence of internal diffusion resistance (Huang et al., 2018; Xiong et al., 2018). Previously, many positive environmental effects of Fe (hydr)oxide NPs have been found, such as stimulating *Vigna radiata* growth, promoting the soil microbial metabolic activity and nitrification potential, increasing some enzyme activities, and improving some microbial growth and abundances (He et al., 2011, 2016; Ren et al., 2018b).

Composting has been widely used for treatment of a variety of wastes, such as agricultural waste, sewage sludge, bio-waste, and feces (Ye et al., 2017a; Zhang et al., 2015). Pathogens are destroyed and biodegradable components are decomposed into sanitary, stable and humus-like substances during composting, resulting in good fertilizers and conditioners for soil (Gao et al., 2019; Ren et al., 2018c). Ecologically, composting is a biological process completed by the combined activities of various microbes which involved in all events of organic matter (OM) biotransformation (Awasthi et al., 2018; Wei et al., 2019). It was found that AgNPs could improve nitrogen conservation by affecting functional enzyme activities and genes abundances during composting (Zhang et al., 2017; Zeng et al., 2018). Higher carbon mineralization rates were detected during composting amended with AgNPs or Ag-based NPs (Stamou and Antizar-Ladislao, 2016). It has also been reported that bacterial community structure was changed during composting in the presence of AgNPs (Gitipour et al., 2013). Most of existing researches on NPs in the field of composting were focused on the effects of Ag or Ag-based NPs, so more kinds of NPs need to be further studied. Additionally, the impacts of NPs on different microbial populations (e.g. bacteria, fungi and actinomycetes) have not yet been well understood. As these microbes are possibly sensitive to environmental variables (Qin et al., 2018; Zhang et al., 2018b), it is also important to evaluate the relationships between changes of microorganisms and environmental variables.

So, inspired by the aforementioned positive environmental impacts of Fe (hydr)oxide NPs and the research status of nanomaterials in the field of composting, we aimed to investigate the different evolutions of bacteria, fungi and actinomycetes during agricultural waste composting which was added with nanohematite and nanomagnetite as amendments. Driving factors of microbial abundances (bacteria, fungi, actinomycetes) were identified using redundancy analysis (RDA). Another novelty was that partial least-squares path modeling (PLS-PM), which was a powerful statistical method of multivariate data sets but rarely used in analyzing relationships between microorganisms and parameters in composting field, was performed in this study to further explore the direct, indirect and total effect of the significant variables. Partial RDA was also conducted to evaluate the specific contribution of each significant factor to each microbial abundance in different treatments. This study will greatly enrich the information about influences of NPs on microorganisms during composting.

2. Materials and methods

2.1. Materials preparation

Nanohematite with average size of 8.7 nm was prepared by method of forced hydrolysis of Fe $(NO_3)_3{\cdot}9H_2O$ solution, as reported by Barton et al. (2011). Firstly, 1 M Fe $(NO_3)_3{\cdot}9H_2O$ solution (60 mL) was added into the boiling ultrapure water (750 mL) drop by drop under a condition of vigorous stirring. The solution was then cooled to room temperature. After dialysis of the above mixture, the particles were stored in suspensions at 4 °C in dark.

Nanomagnetite with average size of 15.6 nm was synthesized using the method by a previous literature (Jiang et al., 2014) with modifications. A 200-mL solution containing 8.5 g $FeSO_4{\cdot}7H_2O$ and 12.3 g $FeCl_3{\cdot}6H_2O$ was heated to 90 °C in a three-necked flask which was equipped with a reflux condenser. The whole heating process proceeded with continuously stirring. Then, 30 mL ammonium hydroxide solution (25%) was rapidly added into the flask and the mixture was kept stirring at 90 °C for another hour. Finally, the mixture was cooled to room temperature and the black nanomagnetite was prepared for use after being washed several times with ultrapure water.

The raw composting materials, including rice straw, vegetable waste, soil, and bran, were collected as described in our previous studies (Zhang et al., 2015). Pretreatments of the raw materials were performed, in which rice straw and vegetable were naturally air-dried and chopped into a length of 1.5 cm, and the soil which was used for enrichment of microbes was sifted using a 60-mesh standard sieve to get rid of debris. The physico-chemical characteristics of each raw composting material could be seen in Supplementary Material.

2.2. Experiment settings and sample collection

Laboratory experiments were conducted in boxes with a capacity of 65 L and lasted for two months. Three different treatments were set up in this research as follows: T-control was the one without any addition, and T-nanohematite and T-nanomagnetite were added with nanohematite and nanomagnetite at 10 mg/kg compost, as He et al., (2016) indicated that Fe (hydr)oxide NPs at this concentration promoted microbial activity. The raw materials, namely rice straw, vegetable, soil and bran, were blended evenly at a weight ratio of 30:8:27:5. Moisture content and C/N of the mixture were adjusted to about 55% and 30, respectively. Good aerobic conditions were provided by daily turning during the first two weeks and turning on each sampling day afterwards. Subsamples were gathered and homogenized from different locations of the heaps, then stored at 4 °C and −20 °C for analysis of physico-chemical parameters and molecular biology, respectively.

2.3. Physico-chemical analysis

Pile temperature was recorded using a thermometer from the upper, middle, and bottom layer. Moisture content was determined by drying the fresh samples at 105 °C for 24 h until a constant weight. pH was determined by shaking compost samples with ultrapure water at a weight/volume (w/v) ratio of 1:10 under 200 rpm for 40 min, and then the filtered supernatant was determined using a digital pH meter. NH_4^+-N and NO_3^--N were extracted by shaking the compost samples with 2 M of KCl solution at a ratio of 1:50 (w/v) under 150 rpm for 1 h and determined by flow injection analysis (AA3, Germany). Mineral N equals to the sum of NH_4^+-N and NO_3^--N. Samples for TN determination were dried and milled before determination using an elemental analyzer (Elementar, Vario Max CN, Germany). The OM content was determined by combusting the ground dry samples at 550 °C for 6 h in a muffle furnace. Subsequently, the total organic carbon (TOC) was calculated referring to previous literature (Zhang et al., 2018b). Samples for water soluble carbon (WSC) determination which was performed on Total Organic Carbon Analyzer (TOC-5000A, Shimadzu, Japan) were

shaken with ultrapure water (1:10, w/v) at 200 rpm for 40 min. Then the supernatant was cleared by filtering through ordinary filter paper and 0.45 μm filter membrane. C/N is the ratio of TOC to TN.

2.4. Total genomic DNA extraction and quantification of microorganisms

The genomic DNA was extracted from 0.35 g of triplicate samples referring to the manufacturer's instruction of E.Z.N.A. ®Soil DNA Kit (OMEGA Bio-Tek, Inc., Norcross, GA, USA). Then the concentration and quality of DNA were determined using spectrophotometer (NanoDrop, Thermo Scientific, Wilmington, DE, USA).

The abundances of bacteria, fungi, and actinomycetes were quantified by the method of qPCR. First of all, DNA samples which were used as the template were 10-fold diluted to eliminate the inhibition of humus-like substances to qPCR reaction (Ye et al., 2017b). All the amplifications were performed in triplicate on the iCycler IQ5 Thermocycler (Bio-Rad, USA) in 20 μL reaction mixtures consisting of 10 μL 2 × SuperRedal PreMix Plus (SYBR Green I), 2 μL diluted DNA, 0.4 μL each primer, and 7.2 μL ddH_2O. Negative controls without DNA template were included in parallel. The specific amplification procedures and primer sequences were shown in Supplementary material. Standard curves with linearity of $R^2 > 0.99$ were generated according to the qPCR results of serial 10-dilution of standards. Finally, the microbial abundances were presented as copies/kg compost based on dry weight.

2.5. Evaluation of relationships between microbial abundances and physico-chemical parameters

The multivariate relationships between microbial abundances and environmental variables were analyzed using Canoco 4.5. Firstly, detrended correspondence analysis (DCA) was done to determine which model was better for analysis of these microbial abundances. Results showed that the maximum length of DCA ordinate axis was less than 3, indicating that the unimodal model was not suitable. Consequently, a linear model, redundancy analysis (RDA), was chosen to ordinate the changes of microbial abundance to environmental variables (Li et al., 2019). The relationships between microbial abundances and variables were visualized via ordination triplots which were created by Cano-Draw for Windows. Manual forward selection was conducted to identify the significant factors. Partial RDA was used to evaluate the individual contribution of each significant factor to each microbial abundance (i.e., bacteria, fungi and actinomycetes) by eliminating the influences of other significant ones. Monte Carlo test with 999 unrestricted permutations was complemented to test the significance level ($P < 0.05$) of the first canonical axis and all canonical axes.

Partial least-squares path modeling [PLS-PM, the R package plspm (v 0.4.9)] was applied to further investigate the direct, indirect, and interactive effects of all measured environmental variables on microbial abundances. It is an excellent statistical method to explore the interactive associations between observed and latent variables, and is widely employed to determine and predict relationships among multivariate data sets (Liao et al., 2018). The following variables were included in this model: composting physico-chemical parameters (i.e., pile temperature, pH, moisture content, NH_4^+-N, NO_3^--N, TN, OM, TOC, WSC, C/N), microbial abundances (i.e., bacteria, fungi, actinomycetes). Indirect effects were expressed as the coefficients of multiplied paths that link response variables with predictor variables including all potential paths except the direct effect. The goodness of fit (GoF) was used as a judgment of the overall predictive power in the model. All data of physico-chemical parameters and microbial abundances were standardized to eliminate the influence of different magnitudes on the multivariate analysis.

2.6. Data analyses

All determinations were performed in triplicate and mean values were presented. One-way analysis of variance (ANOVA) by SPSS 19.0 was used to test the difference between mean values under a 95% confidence level.

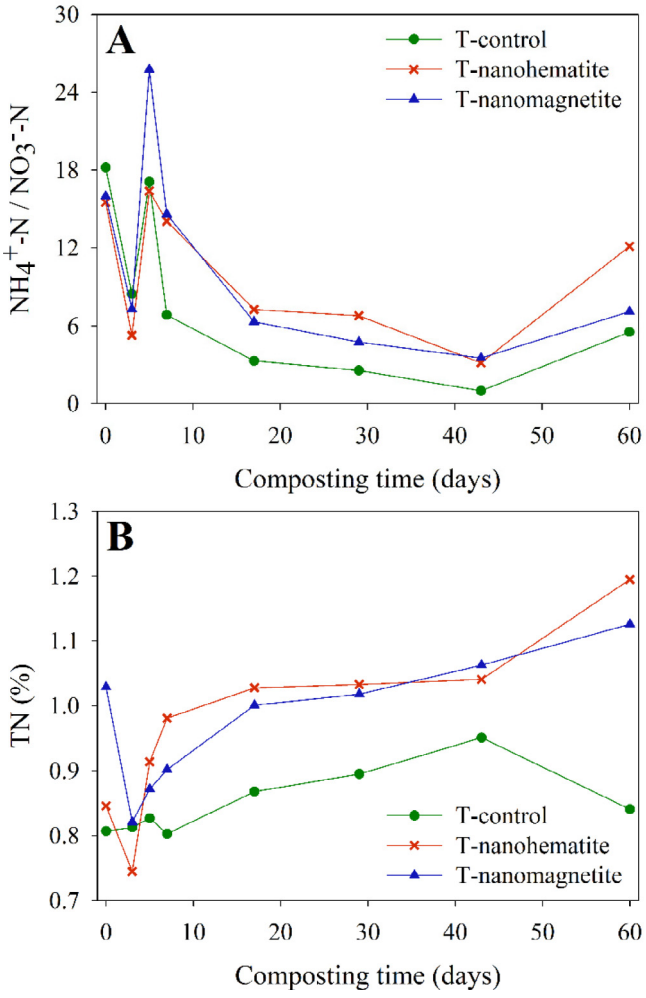

Fig. 1. Changes of (A) NH_4^+-N/NO_3^--N ratio and (B) TN content during composting.

3. Results and discussion

3.1. Temperature evolution during composting

A good thermophilic phase (> 50 °C) lasting about 7 days is important to effectively kill the pathogenic microorganisms and produce hygienic compost, thereby meeting the sanitary requirements of Chinese National Standard. Huang et al. (2017) reported that temperature higher than 55 °C for at least three days is extremely necessary to destroy the weed seeds and pathogens. In this study, the thermophilic phase lasted 8 days and temperature above 55 °C maintained 5–8 days (Supplementary material). Therefore, the pile temperatures of all treatments met the requirements for producing sanitary compost.

The three treatments displayed identical temperature patterns: mesophilic, thermophilic, cooling and maturity phase. All the pile temperatures increased rapidly and reached thermophilic phase within 3 days due to the production of energy via intensive decomposition of easily available OM by microorganisms to stimulate their growth and activity (Yuan et al., 2016). The phase (> 55 °C) was longer in piles treated with Fe (hydr)oxide NPs than T-control. While the peak value in T-nanomagnetite was the lowest compared with other two treatments. An explanation for these phenomena would be that iron is a necessary

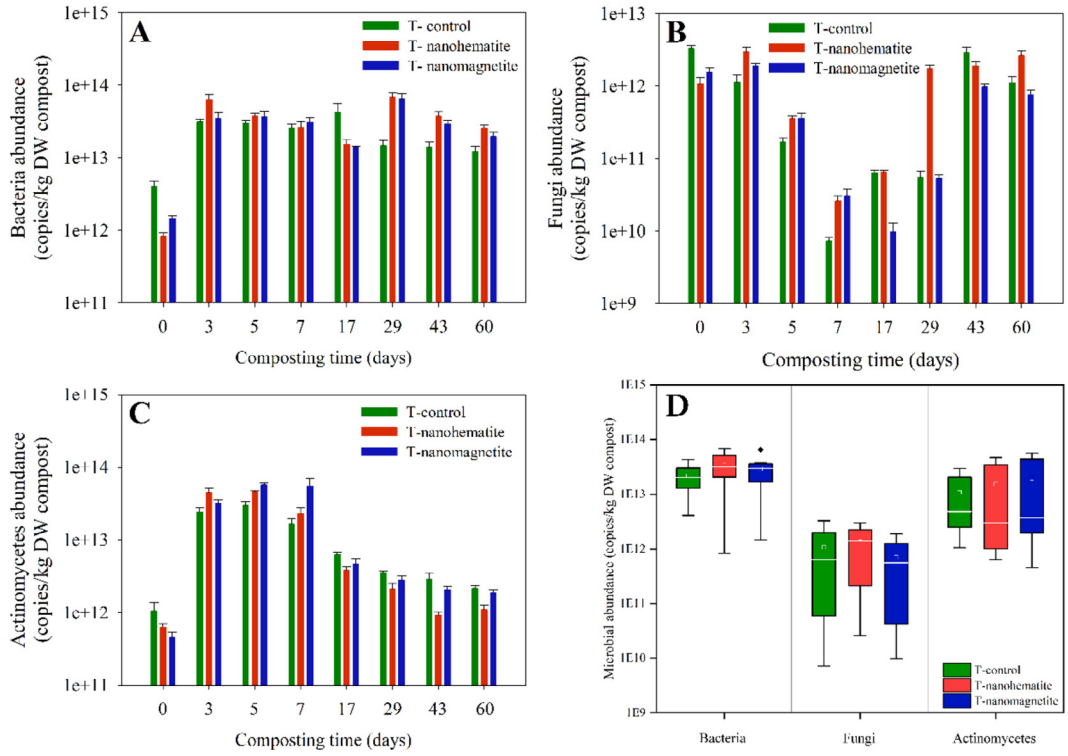

Fig. 2. Changes of microbial abundances during composting. (A) Bacteria; (B) Fungi; (C) Actinomycetes; (D) Box plot of each microbial abundance. The upper and lower borders of box represent the upper and lower quartile, respectively. The white lines and small boxes inside represent median and mean value, respectively. The whiskers represent minimum and maximum value.

nutrient for most microbes, while the positive effect of iron in magnetite NPs was weakened by the reactive oxygen species which was generated via release of Fe^{2+} (He et al., 2011; Tang et al., 2018). The significant higher temperatures in treatments with Fe (hydr)oxide NPs around the day 10 indicated that the amendment of Fe (hydr)oxide NPs might stimulate the degradation of OM which was relatively difficult to degrade, thus generating more heat. While the reason for significant higher temperature ($P < 0.05$) in T-control during day 17–43 might be that the available OM in T-control decreased more slowly during the earlier stage than Fe (hydr)oxide NPs treatments, thus there were more easily degradable OM in T-control during day 17–43 to maintain higher temperature in this phase.

3.2. NH_4^+-N/NO_3^--N ratio and TN during composting

The NH_4^+-N/NO_3^--N ratio is always acknowledged as a nitrification index during composting. As presented in Fig. 1A, the profiles of NH_4^+-N/NO_3^--N ratio in all treatments decreased in the first 3 days which might be ascribed to nitrification during mesophilic phase. With the temperature rising, the ratio correspondingly increased to the peak value on day 5 as the growth and activity of nitrifying bacteria were inhibited by the high temperature (Awasthi et al., 2017). A previous study once indicated that nitrification was inhibited when the temperature was above 40 °C (Sánchez-Monedero et al., 2001). While in this study, the NH_4^+-N/NO_3^--N ratio still decreased during day 5 to 10 when the temperature was above 40 °C, and this might be due to the emission of NH_3 under high temperature. As can be seen in Fig. 1A, the content of NH_4^+-N was relatively higher than that of NO_3^--N in all treatments throughout composting process, this was also reported by other researches (Jiang et al., 2015). The higher NH_4^+-N/NO_3^--N ratio in T-nanohematite and T-nanomagnetite indicated that the nitrification might be weakened by the amendment of Fe (hydr)oxide NPs, subsequently resulting in more mineral N retention and the mineral N was mainly in the form of NH_4^+-N in the final compost (Supplementary material), which might improve the nitrogen use efficiency of the final compost since NO_3^--N was easily lost through leaching, run-off, and denitrification when the compost was reused in agriculture (Qiao et al., 2015). An NH_4^+-N/NO_3^--N ratio less than 0.16 was once considered as a maturity indicator of composting (Bernal et al., 1998). While in this study, the final NH_4^+-N/NO_3^--N ratio was 5.53, 12.14 and 7.11 in T-control, T-nanohematite and T-nanomagnetite, respectively. Zhu (2007) suggested that the final NH_4^+-N/NO_3^--N ratio of mature compost was different with different composting time, ranging from 5.47 to 48.33. Yuan et al. (2016) also found that the final ratios were ranged from 2.69 to 7.79 which were greater than 0.16, and they proposed that the ratio of NH_4^+-N/NO_3–$^-$N might not be a suitable indicator for evaluating the maturity of compost.

The TN content was correlated with the immobilization of NH_4^+-N and the reduction of weight of dry composting materials caused by OM degradation (Tang et al., 2019; Zhang et al., 2018a). As shown in Fig. 1B, the TN content in T-nanohematite and T-nanomagnetite was decreased in the first 3 days due to the intensive NH_3 emission. Afterwards, although the emission of NH_3 was also intensive in the phases when temperature was high, the TN content still increased gradually. It has been suggested that the TN content would increase as a concentration effect if the net loss of dry mass and degradation rate of organic carbon-containing compounds were faster than nitrogen loss (Chan et al., 2016). At the end of composting, the TN content was ranged as T-nanohematite > T-nanomagnetite > T-control (Fig. 1B), and the TN loss was ranged as T-control > T-nanomagnetite > T-nanohematite (Supplementary material). The possible reason might be that the weakening of nitrification by amendment of Fe (hydr)oxide NPs resulted in more TN retention in compost mainly as NH_4^+-N which would improve the nitrogen use efficiency of the final compost (Qiao et al., 2015). The weakening of nitrification might also reduce the nitrogen gases loss which were released during nitrification. Moreover, lower NO_3^--N might reduce the substrate for denitrification, thus lessening TN loss as NO, N_2O and N_2. Compared with previous studies that

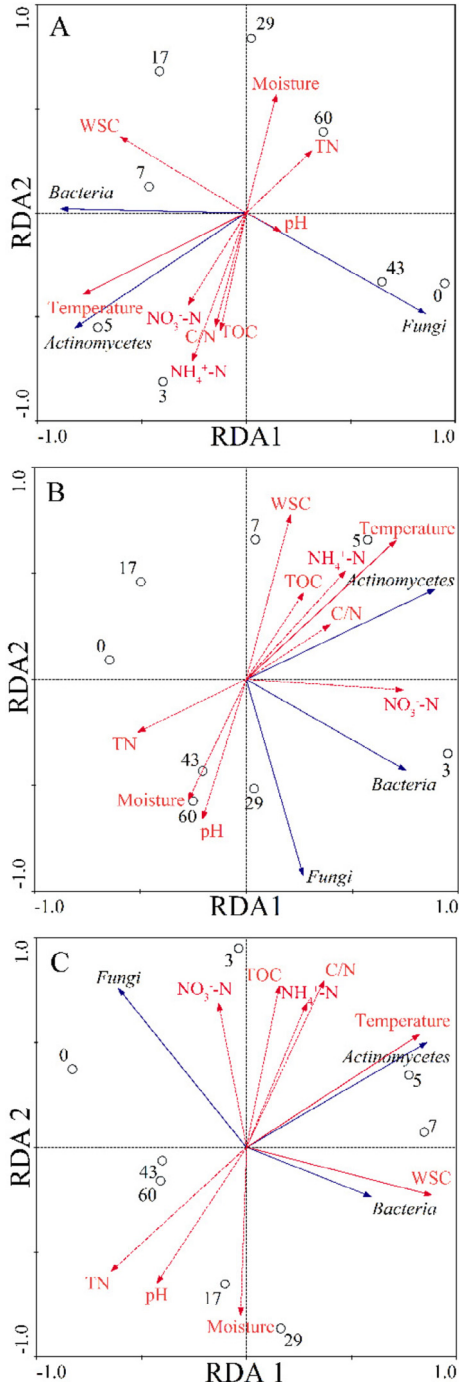

Fig. 3. Redundancy analysis triplot of microbial abundances and environmental variables in (A) T-control; (B) T-nanohematite; (C) T-nanomagnetite. Environmental variables are denoted using red lines and the significant ones are indicated by the red solid lines. Microbial abundances were denoted using blue solid lines. The circles and numbers around represent samples and the corresponding sampling day, respectively. (For interpretation of the references to colour in this figure legend, the reader is referred to the web version of this article.)

researched the impact of AgNPs at a concentration of 10 mg/kg compost (Zeng et al., 2018), the amendment of Fe (hydr)oxide NPs was more effective to reduce the TN loss.

3.3. Evolutions of microbial populations during composting

Changes in microbial abundances during composting are likely to reflect the composting performance. The calculated qPCR efficiencies for bacteria, fungi and actinomycetes were 103.6%, 97.4% and 103.5%, respectively. As shown in Fig. 2, both the bacteria and actinomycetes abundances exhibited similar trends in all treatments throughout the composting process, which showed significant increases ($P < 0.01$) in the first 3 days. Particularly, the number of actinomycetes showed a significant increase in the first 5 days and then decreased regularly until the end of composting. While different from bacteria and actinomycetes in all treatments, the fungi abundances decreased significantly ($P < 0.01$) during the first 7 days and then increased afterwards ($P < 0.01$). A possible reason might be that fungi lost their competitive advantage for nutrients and easily biodegradable OM when competing with bacteria and actinomycetes in the early phase of composting. It was reported that bacteria was the dominant group for the initial degradation of OM and generation of heat during the early stage of composting (Awasthi et al., 2014). With the depletion of easily degradable OM, the resting component mainly consisted of lignocellulose which was difficult to degrade, leading to the decreases of activity and abundance of bacteria and actinomycetes, while the abundances of fungi began to increase at this stage. Previous studies suggested that fungi were the predominant organisms responsible for lignocellulose degradation by secreting extracellular enzymes, such as hydrolytic enzymes, cellulolytic and hemicellulolytic enzymes and ligninolytic enzymes (Bohacz 2017). Consequently, the succession of fungi abundance was opposite to that of bacteria and actinomycetes in the present study.

As shown in Fig. 2A, the abundances of bacteria in T-nanohematite and T-nanomagnetite were higher than that of T-control during most time of composting with the order of T-nanohematite > T-nanomagnetite > T-control. Especially at the maturation phase, the bacteria abundances in treatments with Fe (hydr)oxide NPs were significant higher than that in T-control ($P < 0.01$). As for fungi, the average abundance was in the order of T-control > T-nanohematite > T-nanomagnetite in the first 7 days and it was changed to T-nanohematite > T-control > T-nanomagnetite afterwards (Fig. 2B). Anyway, both the average abundances of bacteria and fungi in T-nanohematite were the highest compared with other two treatments. This was also proved by the box plot (Fig. 2D), which indicated that the average abundances, estimated median as well as the upper and lower quartiles of bacteria and fungi abundances in T-nanohematite were the greatest. It was followed orderly by T-nanomagnetite and T-control for bacteria, and T-control and T-nanomagnetite for fungi. Similar results were found by previous study which indicated that Fe (hydr)oxide NPs increased bacteria and fungi abundances though the effects were not significant (He et al., 2016). The actinomycetes in treatments with Fe (hydr)oxide NPs were significant higher than T-control ($P < 0.05$) during the first 7 days, and significant lower than T-control ($P < 0.05$) afterwards with the lowest value in T-nanohematite (Fig. 2C). However, the average abundances as well as the estimated upper quartiles of actinomycetes were in the order of T-nanomagnetite > T-nanohematite > T-control (Fig. 2D), which might be due to the compensation by the greatly higher abundances during the first 7 days. On the whole, positive effects were induced with the amendment of Fe (hydr)oxide NPs, especially nanohematite.

3.4. Relationships between microbial abundances and physicochemical parameters

RDA analysis was performed to investigate the relationships between the microbial abundances and composting variables. Accordingly, 92.9%, 90.5% and 85.7% of the variation in microbial abundances in T-control, T-nanohematite and T-nanomagnetite were explained by the first two axes (Fig. 3). Manual forward selection showed that temperature was the most significant factor driving the variation of microbial abundances in all treatments, and WSC was another one in T-nanomagnetite. Consequently, to explore effect of the most important factor (temperature) and other variables on microbial

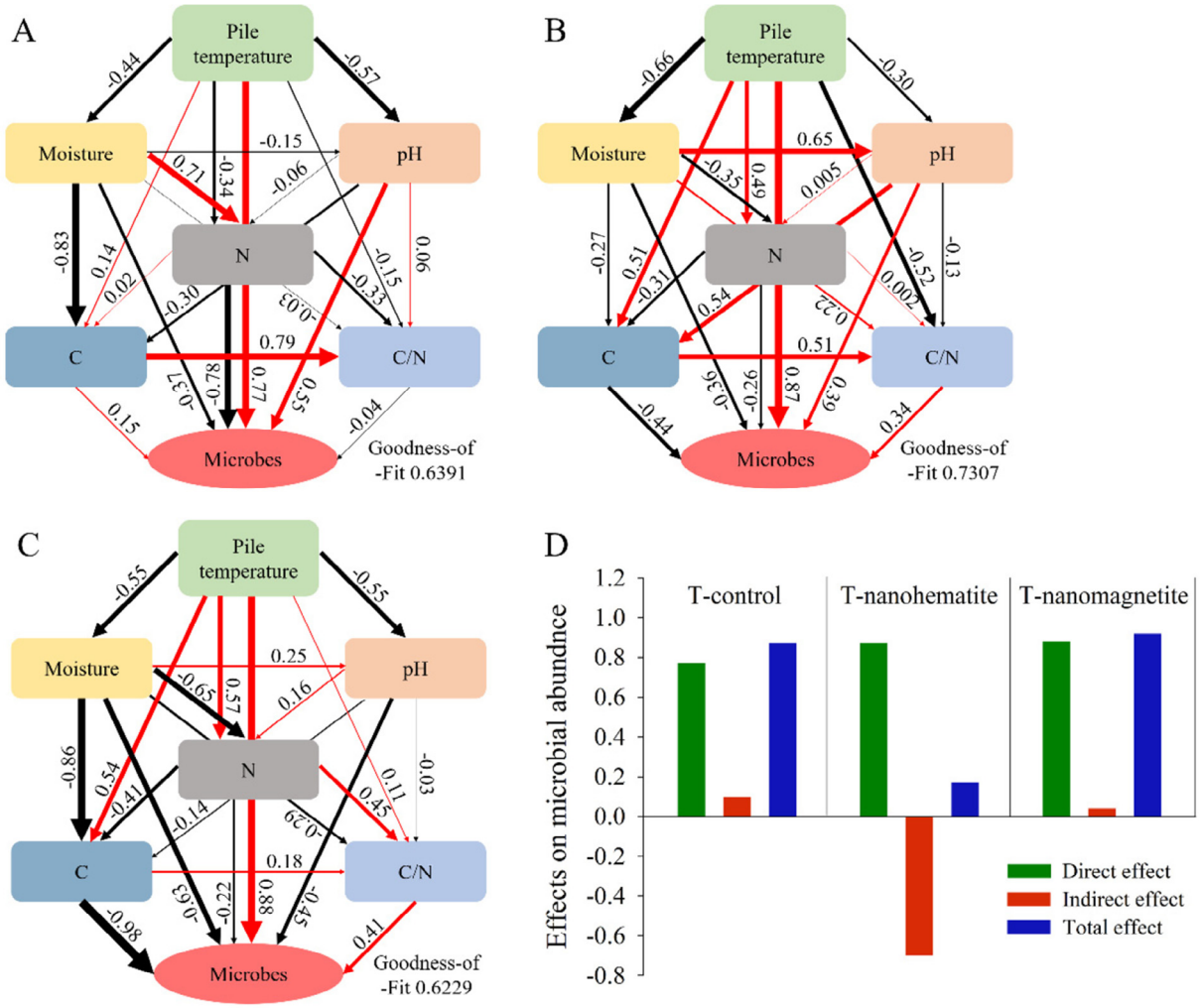

Fig. 4. Partial least squares-path models of different treatments (A) T-control; (B) T-nanohematite; (C) nanomagnetite. Wider arrows indicate greater path coefficients, and red and black colors represent positive and negative effects, respectively. The variable N includes NH_4^+-N, NO_3^--N and TN, and the variable C includes total organic carbon and water soluble organic carbon. (D) Detailed effect of temperature, including direct, indirect and total effect, on microbial abundances in different treatments. (For interpretation of the references to colour in this figure legend, the reader is referred to the web version of this article.)

Table 1
Results of partial RDA indicating the individual influence of the significant variables on each microbial abundance.

Treatments	Microbes	Significant variables	Eigenvalues	Sole explanation	F value	P value
T-control	Fungi	WSC	0.485	48.5%	5.651	0.061
	Actinomycetes	Temperature	0.924	92.4%	91.647	0.003
		pH	0.118	11.8%	11.757	0.019
		Together	0.950	95.0%	47.117	0.003
T-nanohematite	Fungi	WSC	0.555	55.5%	7.492	0.012
	Actinomycetes	Temperature	0.704	70.4%	270.725	0.002
		pH	0.022	2.2%	8.348	0.053
		WSC	0.097	9.7%	37.297	0.003
		Together	0.990	99.0%	126.826	0.001
T-nanomagnetite	Fungi	WSC	0.744	74.4%	30.005	0.001
		C/N	0.285	28.5%	11.490	0.022
		Together	0.876	87.6%	17.667	0.011
	Actinomycetes	Temperature	0.942	94.2%	396.674	0.001
		NO_3^--N	0.016	1.6%	6.801	0.033
		Together	0.988	98.8%	208.156	0.001

abundances in more detail, a PLS-PM was constructed to evaluate the direct and indirect effects between indicators and latent constructs.

Generally, it was found that temperature had similar direct positive effects on variations of microbial abundances in all treatments with value of 0.77, 0.87 and 0.88 in T-control, T-nanohematite and T-nanomagnetite (Fig. 4A-4C), respectively. The indirect positive effect by the correlations between composting temperature and other environmental variables in T-control and T-nanomagnetite raised the total influence of temperature to 0.87 and 0.92, respectively (Fig. 4D). While in T-nanohematite, the total effect of temperature was reduced to 0.18

by the negative indirect effect. A similar result was also presented in a previous study which found that the total effect of temperature was reduced by an offset between the direct positive and indirect negative effect (Liao et al., 2018). From Fig. 4A-4C, it could be seen that all the composting properties shared direct or indirect, positive or negative correlations between each other. Temperature is one of the most influential variables in composting efficiency. In fact, composting is a biological process driven by microorganisms whose successions in community structure and abundance correspond to temperature evolution (Ren et al., 2018a). Our models indicated that the underlying mechanisms causing variations in microbial abundances were different in all treatments.

While Fe (hydr)oxide NPs might also brought direct effects on microbial abundances or indirect effects. For example, it was once reported that dehydrogenase activity (DHA) was positively influenced by Fe (hydr)oxide NPs (He et al., 2011). DHA can reflect the real performance of biological process during composting in terms of OM degradation. And the degradation of OM can affect the parameters during composting, such as temperature, pH, etc. While the microbes are easily affected by changes of environmental parameters. So, it is difficult to distinguish the direct or indirect effect by Fe (hydr)oxide NPs. But anyway, the changes of relationships between microbial abundances and parameters in different treatments might be caused by the amendment of Fe (hydr)oxide NPs.

To further investigate the specific influence of significant factors on each microbial abundance, partial RDA was conducted after manual forward selection with 999 of Monte Carlo Permutation Tests during RDA analysis between each microbial abundance and environmental variables (Table 1). Accordingly, it was found that there were no significant factors driving the changes of bacterial abundances in all treatments. Of course, this just meant that the variations of bacterial abundance were mainly driven by the inter-correlation between different parameters rather than by individual factor, which was in agreement with a previous study (Xi et al., 2016). During forward selection, WSC was found to be the significant factor ($P < 0.05$) affecting fungi abundances in all treatments, with a single explanation of 48.5% ($P = 0.061$), 55.5% ($P = 0.012$), 74.4% ($P = 0.001$) of the variations in T-control, T-nanohematite and T-nanomagnetite, respectively (Table 1). WSC is an easily degradable OM and is generally used as one of the biologically active parameters for evaluation of compost stability, and it is an important factor shaping microorganisms (Zhang et al., 2017). It was also found in a previous study that WSC significantly explained the variation of fungal community (Zhang et al., 2011). While the single explanation of WSC in T-control was not significant any more ($P = 0.061$) during partial RDA, this might indicate that it contributed to fungi mainly through cooperation with other parameters in T-control.

Additionally, temperature was the most significant factor correlated with the changes of actinomycetes abundances in all treatments with sole contribution of 92.4% ($P = 0.003$), 70.4% ($P = 0.002$), 94.2% ($P = 0.001$) of variations in T-control, T-nanohematite, and T-nanomagnetite, respectively. This was similar with an existing literature that found the temperature was the only significant factor correlated with the variation of actinomycetes community (Wang et al., 2014). While in our present study, temperature was not the only factor which significantly affected the actinomycetes. As shown in Table 1, WSC and NO_3^--N was another significant one in T-nanohematite and T-nanomagnetite, respectively. Interestingly, pH as a critical variable influencing the actinomycetes in manual forward selection was found to be not significant in partial RDA ($P = 0.053$) in T-nanohematite, indicating that pH also contributed to the changes of actinomycetes abundances mainly via cooperation with other variables. The fact that the total contributions by all significant factors were greater than a single one suggested that the inter-relationship between these significant factors was also influential to the succession of microorganisms, as also proposed in our previous study (Zhang et al., 2018b). The implication of partial RDA as well as the direct and indirect effects of parameters on the successions of microbial abundances detected in PLS-PM model supported each other, which indicated complex relationships between different composting parameters.

4. Conclusion

The amendment of Fe (hydr)oxide NPs, especially nanohematite induced positive effects on the average abundances of bacteria and fungi. As the most significant factor, temperature showed similar direct effects on microbes in all treatments. Its total effects increased in T-control and T-nanomagnetite because of the indirect positive effects, while decreased in T-nanohematite by the indirect negative effect. Interactive relationships among multivariate parameters were observed and they differed with different treatments. Additionally, the significant factors for each microbial population and their single contributions were different. Actinomycetes was likely to be more sensitive to the parameters than bacteria and fungi.

Acknowledgements

This research was financially supported by the National Natural Science Foundation of China (51521006, 51378190, 51879100, 51408219) and the Program for Changjiang Scholars and Innovative Research Team in University (IRT-13R17).

Appendix A. Supplementary data

Supplementary data to this article can be found online at https://doi.org/10.1016/j.biortech.2019.121697.

References

Asadishad, B., Chahal, S., Akbari, A., Cianciarelli, V., Azodi, M., Ghoshal, S., Tufenkji, N., 2018. Amendment of agricultural soil with metal nanoparticles: effects on soil enzyme activity and microbial community composition. Environ. Sci. Technol. 52, 1908–1918.

Awasthi, M.K., Awasthi, S.K., Wang, Q., Wang, Z., Lahori, A.H., Ren, X.N., Chen, H.Y., Wang, M.J., Zhao, J.C., Zhang, Z.Q., 2018. Influence of biochar on volatile fatty acids accumulation and microbial community succession during biosolids composting. Bioresour. Technol. 251, 158–164.

Awasthi, M.K., Pandey, A.K., Khan, J., Bundela, P.S., Wong, J.W.C., Selvam, A., 2014. Evaluation of thermophilic fungal consortium for organic municipal solid waste composting. Bioresour. Technol. 168, 214–221.

Awasthi, M.K., Wang, Q., Chen, H.Y., Wang, M.J., Ren, X.N., Zhao, J.C., Li, J., Guo, D., Li, D.S., Awasthi, S.K., Sun, X.N., Zhang, Z.Q., 2017. Evaluation of biochar amended biosolids co-composting to improve the nutrient transformation and its correlation as a function for the production of nutrient-rich compost. Bioresour. Technol. 237, 156–166.

Barton, L.E., Grant, K.E., Kosel, T., Quicksall, A.N., Maurice, P.A., 2011. Size-dependent Pb sorption to nanohematite in the presence and absence of a microbial siderophore. Environ. Sci. Technol. 45, 3231–3237.

Bernal, M.P., Paredes, C., Sánchez-Monedero, M.A., Cegarra, J., 1998. Maturity and stability parameters of composts prepared with a wide range of organic wastes. Bioresour. Technol. 63, 91–99.

Bohacz, J., 2017. Lignocellulose-degrading enzymes, free-radical transformations during composting of lignocellulosic waste and biothermal phases in small-scale reactors. Sci. Total Environ. 580, 744–754.

Chan, M.T., Selvam, A., Wong, J.W., 2016. Reducing nitrogen loss and salinity during 'struvite' food waste composting by zeolite amendment. Bioresour. Technol. 200, 838–844.

Gao, X.T., Tan, W.B., Zhao, Y., Wu, J.Q., Sun, Q.H., Qi, H.S., Xie, X.Y., Wei, Z.M., 2019. Diversity in the mechanisms of humin formation during composting with different materials. Environ. Sci. Technol. 53, 3653–3662.

Gitipour, A., El Badawy, A., Arambewela, M., Miller, B., Scheckel, K., Elk, M., Ryu, H., Gomez-Alvarez, V., Domingo, J.S., Thiel, S., Tolaymat, T., 2013. The impact of silver nanoparticles on the composting of municipal solid waste. Environ. Sci. Technol. 47, 14385–14393.

Gong, J., Wang, B., Zeng, G., Yang, C., Niu, C., Niu, Q., Zhou, W., Liang, Y., 2009. Removal of cationic dyes from aqueous solution using magnetic multi-wall carbon nanotube nanocomposite as adsorbent. J. Hazard. Mater. 164, 1517–1522.

He, K., Zeng, Z., Chen, A., Zeng, G., Xiao, R., Xu, P., Huang, Z., Shi, J., Hu, L., Chen, G., 2018. Advancement of Ag-graphene based nanocomposites: an overview on synthesis and its applications. Small 1800871, 1–13.

He, S.Y., Feng, Y.Z., Ni, J., Sun, Y.F., Xue, L.H., Feng, Y.F., Yu, Y.L., Lin, X.G., Yang, L.Z.,

2016. Different responses of soil microbial metabolic activity to silver and iron oxide nanoparticles. Chemosphere 147, 195–202.
He, S.Y., Feng, Y.Z., Ren, H.X., Zhang, Y., Gu, N., Lin, X.G., 2011. The impact of iron oxide magnetic nanoparticles on the soil bacterial community. J. Soil. Sediment. 11, 1408–1417.
Huang, C., Zeng, G.M., Huang, D.L., Lai, C., Xu, P., Zhang, C., Cheng, M., Wan, J., Hu, L., Zhang, Y., 2017. Effect of *Phanerochaete chysosporium* inoculation on bacterial community and metal stabilization in lead-contaminated agricultural waste composting. Bioresour. Technol. 243, 294–303.
Huang, Z., He, K., Song, Z., Zeng, G., Chen, A., Yuan, L., Li, H., Hu, L., Guo, Z., Chen, G., 2018. Antioxidative response of *Phanerochaete chrysosporium* against silver nanoparticle-induced toxicity and its potential mechanism. Chemosphere 211, 573–583.
Jiang, J.S., Liu, X.L., Huang, Y.M., Huang, H., 2015. Inoculation with nitrogen turnover bacterial agent appropriately increasing nitrogen and promoting maturity in pig manure composting. Waste Manage. 39, 78–85.
Jiang, W.J., Cai, Q., Xu, W., Yang, M.W., Cai, Y., Dionysiou, D.D., O'Shea, K.E., 2014. Cr (VI) adsorption and reduction by humic acid coated on magnetite. Environ. Sci. Technol. 48, 8078–8085.
Li, M., Wu, Q., Wang, Q.W., Xiang, D.D., Zhu, G.N., 2018. Effect of titanium dioxide nanoparticles on the bioavailability and neurotoxicity of cypermethrin in zebrafish larvae. Aquat. Toxicol. 199, 212–219.
Li, M.Y., Ren, L.H., Zhang, J.C., Luo, L., Qin, P.F., Zhou, Y.Y., Huang, C., Tang, J.Y., Huang, H.L., Chen, A.W., 2019. Population characteristics and influential factors of nitrogen cycling functional genes in heavy metal contaminated soil remediated by biochar and compost. Sci. Total Environ. 651, 2166–2174.
Liao, H.P., Lu, X.M., Rensing, C., Friman, V.P., Geisen, S., Chen, Z., Yu, Z., Wei, Z., Zhou, S.G., Zhu, Y.G., 2018. Hyperthermophilic composting accelerates the removal of antibiotic resistance genes and mobile genetic elements in sewage sludge. Environ. Sci. Technol. 52, 266–276.
Qiao, C.L., Liu, L.L., Hu, S.J., Compton, J.E., Greaver, T.L., Li, Q.L., 2015. How inhibiting nitrification affects nitrogen cycle and reduces environmental impacts of anthropogenic nitrogen input. Global Change Biol. 21, 1249–1257.
Qin, L., Zeng, G., Lai, C., Huang, D., Xu, P., Zhang, C., Cheng, M., Liu, X., Liu, X., Li, B., Yi, H., 2018. "Gold Rush" in modern science: fabrication strategies and typical advanced applications of gold nanoparticles in sensing. Coordin. Chem. Rev. 359, 1–31.
Ren, L., Cai, C., Zhang, J., Yang, Y., Wu, G., Luo, L., Huang, H., Zhou, Y., Qin, P., Yu, M., 2018a. Key environmental factors to variation of ammonia-oxidizing archaea community and potential ammonia oxidation rate during agricultural waste composting. Bioresour. Technol. 270, 278–285.
Ren, X., Zeng, G., Tang, L., Wang, J., Wan, J., Feng, H., Song, B., Huang, C., Tang, X., 2018b. Effect of exogenous carbonaceous materials on the bioavailability of organic pollutants and their ecological risks. Soil Biol. Biochem. 116, 70–81.
Ren, X., Zeng, G., Tang, L., Wang, J., Wan, J., Liu, Y., Yu, J., Yi, H., Ye, S., Deng, R., 2018c. Sorption, transport and biodegradation-An insight into bioavailability of persistent organic pollutants in soil. Sci. Total Environ. 610–611, 1154–1163.
Sánchez-Monedero, M.A., Roig, A., Paredes, C., Bernal, M.P., 2001. Nitrogen transformation during organic waste composting by the Rutgers system and its effects on pH, EC and maturity of the composting mixtures. Bioresour. Technol. 78, 301–308.
Stamou, I., Antizar-Ladislao, B., 2016. The impact of silver and titanium dioxide nanoparticles on the in-vessel composting of municipal solid waste. Waste Manage. 56, 71–78.
Tang, J.Y., Zhang, J.C., Ren, L.H., Zhou, Y.Y., Gao, J., Luo, L., Yang, Y., Peng, Q.H., Huang, H.L., Chen, A.W., 2019. Diagnosis of soil contamination using microbiological indices: a review on heavy metal pollution. J. Environ. Manage. 242, 121–130.
Tang, X., Zeng, G., Fan, C., Zhou, M., Tang, L., Zhu, J., Wan, J., Huang, D., Chen, M., Xu, P., Zhang, C., Xiong, W., 2018. Chromosomal expression of CadR on *Pseudomonas aeruginosa* for the removal of Cd (II) from aqueous solutions. Sci. Total Environ. 636, 1355–1361.
Wang, C., Guo, X.H., Deng, H., Dong, D., Tu, Q.P., Wu, W.X., 2014. New insights into the structure and dynamics of actinomycetal community during manure composting. Appl. Microbiol. Biotechnol. 98, 3327–3337.
Wang, Y., Zhu, Y., Hu, Y., Zeng, G., Zhang, Y., Zhang, C., Feng, C., 2018. How to construct DNA hydrogels for environmental applications: advanced water treatment and environmental analysis. Small 14, 1–19.
Wei, Y.Q., Wu, D., Wei, D., Zhao, Y., Wu, J.Q., Xie, X.Y., Zhang, R.J., Wei, Z.M., 2019. Improved lignocellulose-degrading performance during straw composting from diverse sources with actinomycetes inoculation by regulating the key enzyme activities. Bioresour. Technol. 271, 66–74.
Xi, B.D., Zhao, X.Y., He, X.S., Huang, C.H., Tan, W.B., Gao, R.T., Zhang, H., Li, D., 2016. Successions and diversity of humic-reducing microorganisms and their association with physico-chemical parameters during composting. Bioresour. Technol. 219, 204–311.
Xiong, W., Zeng, Z., Li, X., Zeng, G., Xiao, R., Yang, Z., Zhou, Y., Zhang, C., Cheng, M., Hu, L., Zhou, C., Qin, L., Xu, R., Zhang, Y., 2018. Multi-walled carbon nanotube/aminomino-functionalized-53 (Fe) composites: remarkable adsorptive removal of antibiotics from aqueous solutions. Chemosphere 210, 1061–1069.
Xu, C., Peng, C., Sun, L.J., Zhang, S., Huang, H.M., Chen, Y.X., Shi, J.Y., 2015. Distinctive effects of TiO_2 and CuO nanoparticles on soil microbes and their community structures in flooded paddy soil. Soil Biol. Biochem. 86, 24–33.
Xu, P., Zeng, G., Huang, D., Feng, C., Hu, S., Zhao, M., Lai, C., Wei, Z., Huang, C., Xie, G., Liu, Z., 2012. Use of iron oxide nanomaterials in wastewater treatment: a review. Sci. Total Environ. 424, 1–10.
Yang, Y., Zhang, C., Lai, C., Zeng, G., Huang, D., Cheng, M., Wang, J., Chen, F., Zhou, C., Xiong, W., 2018. BiOX (X = Cl, Br, I) photocatalytic nanomaterials: applications for fuels and environmental management. Adv. Colloid Interfac. 254, 77–93.
Ye, S., Zeng, G., Wu, H., Zhang, C., Dai, J., Liang, J., Yu, J., Ren, X., Yi, H., Cheng, M., Zhang, C., 2017a. Biological technologies for the remediation of co-contaminated soil. Crit. Rev. Biotechnol. 37, 1062–1076.
Ye, S., Zeng, G., Wu, H., Zhang, C., Liang, J., Dai, J., Liu, Z., Xiong, W., Wan, J., Xu, P., Cheng, M., 2017b. Co-occurrence and interactions of pollutants, and their impacts on soil remediation-A review. Crit. Rev. Env. Sci. Tec. 47, 1528–1553.
Yi, H., Huang, D., Qin, L., Zeng, G., Lai, C., Cheng, M., Ye, S., Song, B., Ren, X., Guo, X., 2018. Selective prepared carbon nanomaterials for advanced photocatalytic application in environmental pollutant treatment and hydrogen Production. Appl. Catal. B-Environ. 238, 408–424.
Yuan, J., Chadwick, D., Zhang, D.F., Li, G.X., Chen, S.L., Luo, W.H., Du, L.L., He, S.Z., Peng, S.P., 2016. Effects of aeration rate on maturity and gaseous emissions during sewage sludge composting. Waste Manage. 56, 403–410.
Zeng, G.M., Zhang, L.H., Dong, H.R., Chen, Y.N., Zhang, J.C., Zhu, Y., Yuan, Y.J., Xie, Y.K., Fang, W., 2018. Pathway and mechanism of nitrogen transformation during composting: functional enzymes and genes under different concentrations of PVP-AgNPs. Bioresour. Technol. 253, 112–120.
Zhang, D.F., Luo, W.H., Li, Y., Wang, G.Y., Li, G.X., 2018a. Performance of co-composting sewage sludge and organic fraction of municipal solid waste at different proportions. Bioresour. Technol. 250, 853–859.
Zhang, J.C., Zeng, G.M., Chen, Y.N., Yu, M., Yu, Z., Li, H., Yu, Y., Huang, H.L., 2011. Effects of physic-chemical parameters on the bacterial and fungal communities during agricultural waste composting. Bioresour. Technol. 102, 2950–2956.
Zhang, L.H., Zeng, G.M., Dong, H.R., Chen, Y.N., Zhang, J.C., Yan, M., Zhu, Y., Yuan, Y.J., Xie, Y.K., Huang, Z.Z., 2017. The impact of silver nanoparticles on the co-composting of sewage sludge and agricultural waste: evolutions of organic matter and nitrogen. Bioresour. Technol. 230, 132–139.
Zhang, L.H., Zeng, G.M., Zhang, J.C., Chen, Y.N., Yu, M., Lu, L.H., Li, H., Zhu, Y., Yuan, Y.J., Huang, A.Z., He, L., 2015. Response of denitrifying genes coding for nitrite (*nirK* or *nirS*) and nitrous oxide (*nosZ*) reductases to different physic-chemical parameters during agricultural waste composting. Appl. Microbiol. Biotechnol. 99, 4059–4070.
Zhang, L.H., Zhang, J.C., Zeng, G.M., Dong, H.R., Chen, Y.N., Huang, C., Zhu, Y., Xu, R., Cheng, Y.J., Cao, W.C., Fang, W., 2018b. Multivariate relationships between microbial communities and environmental variables during co-composting of sewage sludge and agricultural waste in the presence of PVP-AgNPs. Bioresour. Technol. 261, 10–18.
Zhou, C., Lai, C., Zhang, C., Zeng, G., Huang, D., Cheng, M., Hu, L., Xiong, W., Chen, M., Wang, J., Yang, Y., Jiang, L., 2018. Semiconductor/boron nitride composites: synthesis, properties, and photocatalysis application. Appl. Catal. B-Environ. 238, 6–18.
Zhu, N., 2007. Effect of low initial C/N ratio on aerobic composting of swine manure with rice straw. Bioresour. Technol. 98, 9–13.